# Monitoring stress changes in carbon fiber reinforced polymer composites with GHz radiation

Research Article Vol. 56, No. 22 / August 1 2017 / Applied Optics 6405

applied optics

# Monitoring stress changes in carbon fiber reinforced polymer composites with GHz radiation

PETER SCHEMMEL AND ANDREW J. MOORE*

*Institute of Photonics and Quantum Sciences, Heriot-Watt University, Edinburgh EH14 4AS, UK*
**Corresponding author: a.moore@hw.ac.uk*

*Received 12 April 2017; revised 16 May 2017; accepted 16 May 2017; posted 17 May 2017 (Doc. ID 292340); published 1 August 2017*

**We performed proof of concept experiments to demonstrate that the reflected power of GHz illumination from the surface of carbon fiber reinforced polymer (CFRP) composites is linearly related to the stress in the material. We introduce a stress coefficient to describe the change in normalized power with applied stress, analogous to the stress-optic coefficient, because the effect is attributed to changes in the refractive index of the effective medium comprising the polymer matrix and carbon fibers. Stress coefficients of $-0.549 \pm 0.134$/GPa and $-0.154 \pm 0.024$/GPa were measured for two different composite materials, both linear in the measurement range of 40 MPa and 100 Mpa, respectively. This technique opens up the possibility of non-destructive evaluation of stresses in CFRP components for quality assurance in manufacturing and in structural health monitoring of in-service aerospace and automotive parts.**



***OCIS codes:*** (110.6795) Terahertz imaging; (120.3940) Metrology; (120.4630) Optical inspection; (160.4760) Optical properties.
https://doi.org/10.1364/AO.56.006405

## 1. INTRODUCTION

Carbon fiber reinforced polymers (CFRP) are routinely used in aerospace applications to reduce the reliance on heavier aluminum and titanium alloys [1]. They are also used in automotive applications, particularly motorsport and high-end consumer vehicles [2], in satellites and telescope mirror support systems [3], as well as in construction [4]. Failure of a CFRP component in any of these applications often requires an immediate and expensive repair. Therefore, it is imperative to manufacture high-quality, defect free components, in addition to ensuring that in-service parts maintain their conformity to strict engineering specifications. Controlling residual stresses incurred during manufacture is crucial to this endeavor.

Residual stresses in CFRPs are unavoidable because of the mismatch in thermal expansion coefficients between the carbon fibers and matrix material [5–7]. These stresses must be controlled to ensure that the manufactured component meets the required specifications. This is a well-known problem, and several techniques have been developed to measure stresses in CFPRs [6]. Techniques such as hole drilling [6], measurement of laminate warpage [6,8], embedding strain gauges [9], or x-ray diffraction of embedded metallic powder [10–12] measure residual stresses but require the CFRP to be destroyed or modified in some way. Raman spectroscopy [6,13] and THz time domain spectroscopy [14] can provide information from localized regions to understand the material properties, but they would be prohibitively time-consuming to apply to extended regions for quality control during production. Full-field inspection methods such as optical interferometry [15], acoustic emission [16,17], and visible photoelasticity [18,19] suffer limitations, including the requirement for differential thermal or pressure loading, complicated reconstruction to locate defects, and the need for an optically transparent model of the bulk material containing the carbon fibers, respectively.

The non-destructive testing of CFRPs using radio frequency radiation has been reviewed extensively [20]. Microwaves in the frequency range 8–70 GHz have been used to identify variations in fiber orientation and the position of delaminations, cracks, and dents in CFRPs. The illumination induces eddy currents in the carbon fibers via electromagnetic induction, and a vector network analyzer (VNA) measures variations in the local attenuation and phase of the reflection coefficient. An image showing these local variations in reflection coefficient across the surface can successfully identify regions of interest, but the underlying stress distribution is not quantified.

In this paper, we propose a new non-destructive technique for measuring stresses in CFRPs and show initial experimental results to provide a proof of concept. It is based on a similar technique used to measure stress distributions in bulk ceramics and ceramic thermal barrier coatings [21,22]. We show that measurements of reflected power from the surface of a CFRP object can be used to characterize the internal stress.

This technique has the potential to acquire high-resolution images of the stress distributions in unmodified components via a non-contact method. Therefore, we believe this technique may be better suited to manufacturing environments than current state-of-the-art techniques. The ultimate goal is to develop an instrument that can produce stress images of CFRP parts to detect defects and delaminations during both manufacture and service.

## 2. EXPERIMENTAL SYSTEM

To measure stresses in CFRP specimens, a reflection based plane polariscope was built, utilizing GHz illumination (Fig. 1). A frequency tunable Virginia Diodes synthesizer and amplifier multiplier chain was used to generate a vertically polarized electromagnetic beam with a frequency between 270 and 370 GHz. A pair of plano–convex lenses focused the beam to a spot of 5 mm diameter on to the CFRP specimen, which was mounted in a Deben 2kN tensile testing stage. A second pair of lenses coupled the reflected beam into a pyroelectric detector. In addition, two polarizers were placed on either side of the specimen to ensure that only the vertically oriented portion of the beam was detected.

Each CFRP tensile test specimen was CNC machined in the shape of a tensile testing dogbone from bulk manufactured CFRP sheets [Fig. 2(a)]. The bulk CFRP sheets used in this experiment were "Prepress Carbon Fiber Flat Sheet" supplied by Easy Composites. Each sheet comprised a two-twill weave pattern [Fig. 2(b)] and an epoxy resin matrix material. The dogbones were machined so the carbon fibers in the weave pattern were parallel (and perpendicular) to the loading axis, as indicated in Fig. 2(b). Two different composite types were tested. The first type comprised five 430 g (grams per square meter) carbon fiber layers with one 215 g layer on either side, giving a total thickness of ∼3 mm. The second composite type comprised one 430 g layer with one 215 g carbon fiber layer on either side, giving a total thickness of ∼1 mm.

Measurements were conducted by first mounting the specimen under test in the tensile testing stage, which was balanced so that a 0 N load was initially applied to the specimen.

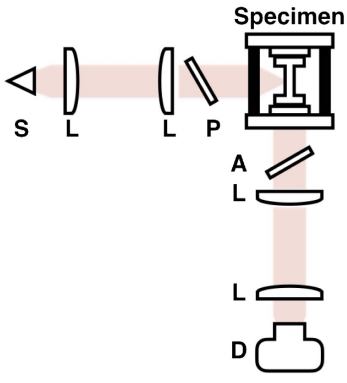


**Fig. 1.** Reflection polariscope showing the GHz beam emitted from the source (S), passing through the plano–convex lens pair (L) and polarizer (P). The tensile testing stage and specimens are angled at 45° to reflect the beam through the analyzer (A) and on to the detector (D).

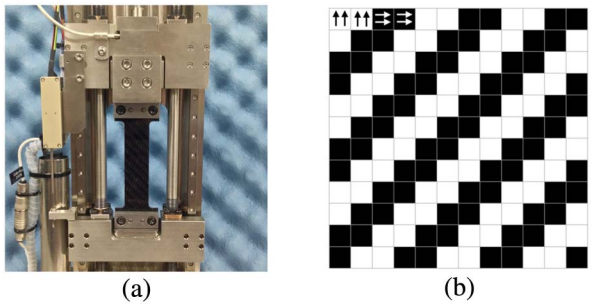


**Fig. 2.** (a) CFRP dogbone specimen in the Deben 2 kN tensile testing stage. (b) A two-twill weave pattern with arrows denoting the orientation of the carbon fibers.

A frequency spectrum was acquired by stepping the source frequency between 270 and 370 GHz, in 0.25 GHz steps, and subsequently recording the reflected power. The applied load was then increased in steps of 200 N up to a maximum load of 1800 N. A frequency spectrum was acquired at each applied load. Spectra acquired in this way were normalized to a background spectrum obtained with the CFRP specimen replaced by an aluminum mirror of the same dimensions in order to remove intensity variations in the source emission and detector response.

Figure 3 shows an example of the normalized reflected power as a function of frequency. Frequency spectra recorded in this manner can be described by the Fresnel equations [23], which enabled changes in the refractive index of bulk ceramics and ceramic thermal barrier coatings to be related to the applied strain in order to determine their direct strain optic coefficient [21,22]. However, because of the complex structure of the CFRP's weave pattern, in addition to the highly absorbing nature of the carbon fibers, a physically representative form of the Fresnel equations could not be found in this case.

To overcome this issue, we measured the average reflected power over the frequency band. The reflected power is a function of several parameters, including the effective refractive index [24–26], surface finish, the polarization state of the

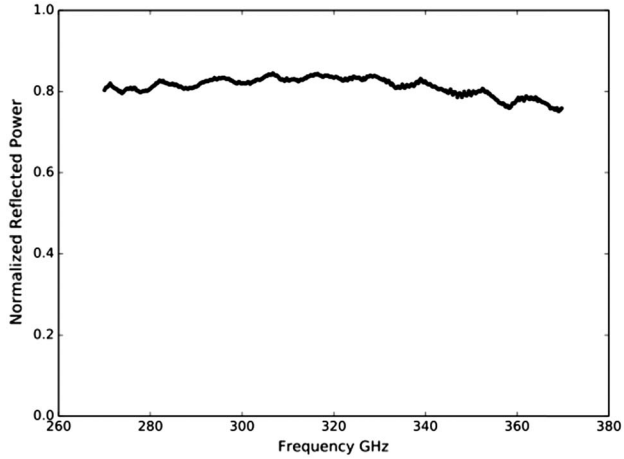


**Fig. 3.** Example of a normalized frequency spectrum between 270 and 370 GHz, recorded from a 3 mm thick CFRP specimen under 1000 N of tensile load.

illumination with respect to the plane of incidence and the direction of the internal carbon fibers, and the absorptivity of the carbon fibers. However, it is expected that these parameters will remain constant as the composite is loaded, with the exception of the effective refractive index if the composite exhibits stress-induced birefringence. We use the effective refractive index to describe the effective medium comprising the polymer matrix and carbon fibers. We have previously measured the stress-induced birefringence in polymers that are opaque at visible wavelengths but that transmit GHz radiation [21]. Therefore, we wished to investigate if measured changes in the reflected power from the CFRP could be calibrated in terms of stress using a relationship of the form

$$\Delta R_p^2 = A\Delta\sigma_1, \tag{1}$$

where $R_p^2 = R_p^* R_p$ is the measured reflected power, $A$ is a constant of proportionality (hereby referred to as the stress coefficient), and $\Delta\sigma_1$ is the change in principle stress in the direction of the plane polarized illumination. We use the stress coefficient rather than the stress-optic coefficient because it is not a property of a general material, but rather the response to stress of a particular composite type. The following section presents results from the experiments to measure the stress coefficient $A$ for the two-till weaved CFRP.

## 3. RESULTS

Three specimens of each composite type were tested three successive times each. We distinguish between these composite types by reference to their thickness, although clearly their mechanical properties do not scale linearly with thickness as they do for a homogeneous material. A normalized frequency spectrum was acquired at each applied load, and the average reflected power across the 270–370 GHz band was determined, as described above. A plot of the average normalized reflected power against applied stress is shown in Figs. 4(a) and 4(b) for the 3 mm and 1 mm thick specimens, respectively. The stress at each load was approximated by dividing the applied load by the initial cross-sectional area of the dogbone specimens. The solid lines show the linear least squares fit to each run, and the average slope of each of these lines is the stress coefficient $A$: $-0.549 \pm 0.134$/GPa and $-0.154 \pm 0.024$/GPa for thick and thin composite types respectively; this is indicated by a dotted line in each figure.

There is an offset between the value of the average normalized reflected power between specimens of the same composite type and to a lesser extent between repeated measurements on the same specimen. However, it is the slope of each line in Figs. 4(a) and 4(b) that is important in calculating the stress coefficient and that is repeatable between specimens and repeated experiments. Figures 4(c) and 4(d) enable the variation in the measured reflected power to be examined for the 3 mm and 1 mm thick composite types, respectively, by removing the offset between individual experiments and the mean without affecting the gradient measured for a given experiment, using a straightforward procedure described in [21]. The mean stress coefficient indicated by the dotted lines in Figs. 4(a) and 4(b) has been repeated in Figs. 4(c) and 4(d).

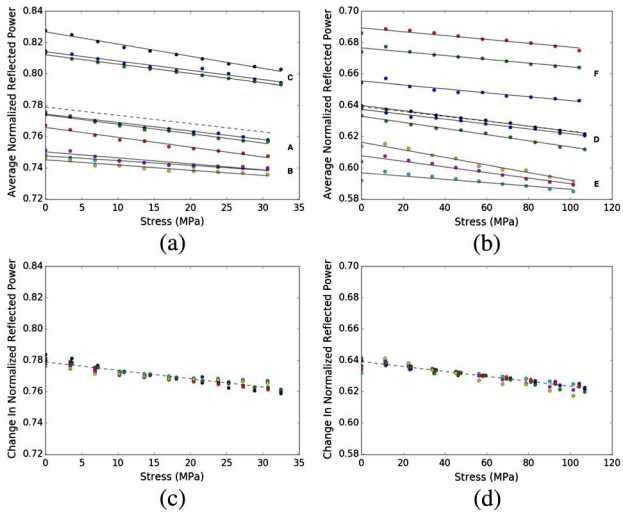


**Fig. 4.** Stress coefficients are calculated from the refractive index versus applied stress for thick (a) and thin (b) composite types, respectively. The absolute offset in reflected power between different specimens of the same thickness is removed to show the scatter for thick (c) and thin (d) composite types. Letter labels denote repeat measurements for a specific sample.

Figures 4(c) and 4(d) indicate the relatively small variation in the stress coefficient measured for a given composite type. However, the stress coefficient is different for the two composite types tested. To emphasize this point, Fig. 5 shows the mean reflected power at each load calculated from the measurement points in Figs. 4(c) and 4(d) with an expanded vertical scale. The maximum reflected power for both composite types has been scaled to unity in order to remove the offset in the reflected power between them. The change in reflected power with applied stress, i.e., the stress coefficient calculated above, is shown by the straight line.

## 4. DISCUSSION

The results in Fig. 4 indicate that it is possible to correlate changes in CFRP stress to the reflected GHz intensity in a

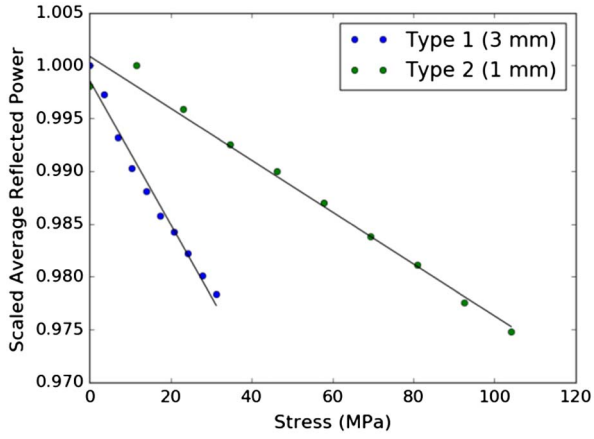


**Fig. 5.** Normalized average reflected power traces for 3 mm and 1 mm thick specimens, scaled to unity for comparison.

plane polariscope. The change in reflected power is attributed to a change in the effective refractive index of the material under load. Other effects, such as surface finish or polarization modulation by the CFPR sheets, may affect the initial reflected power at a given point but are not expected to change under loading. However, the surface finish and internal composite structure are expected to vary across the sheet from which the dogbones specimens were cut, contributing to the offset between the different specimens. Therefore, we have shown that stress states within CFRP sheets may be monitored in a non-destructive manner using reflected GHz illumination.

Figure 5 shows that the magnitude of the stress coefficient differs between different composites. That is to be expected: the different internal structures of the composites mean that the stress is not directly related to the specimen thickness as used in our approximation, although the stress will increase linearly with increasing load. It is also possible that the larger decrease in average reflected power for the thicker composite type implies a larger decrease in the effective refractive index as a function of increased stress, but further research is required to distinguish between these two mechanisms.

The technique presented in this paper treats the matrix and fiber as a single effective medium and therefore measures the combined frequency response. Treating composite materials as a single effective medium has been proposed before [14,24–26], but this is the first time the refractive index and stress-induced birefringence have been used investigate their behavior. Photoelasticity with visible light has only been used to investigate the stress distribution around individual carbon fibers [18,19] within an optically transparent model of the substrate, unlike the full-field birefringence measurements from the effective medium of the real component suggested here.

We are currently investigating how variations in the reflected power can be used to image sub-surface damage and delaminated regions in CFRP sheets. We are particularly interested in attempting to quantify the strain distributions in the CFRP that lead to failure, for which the stress coefficient determined in this paper is the starting point. Even if the stress distributions cannot be quantified by this approach, the variation in the reflected power across the surface should give a qualitative indication of the location of defects over an area that is sufficiently large to be useful in inspection during manufacture and service. Such measurements will require improved spatial resolution, thereby allowing the acquisition of detailed stress images in CFRP components.

## 5. CONCLUSION

This paper has demonstrated a new non-destructive technique to measure stress in CFRP composites by measuring reflected GHz illumination in a plane polariscope. The reflected power was shown to decrease linearly with increasing applied stress for CFRP specimens. The stress coefficient $A$ was measured to be $-0.549 \pm 0.134$/GPa and $-0.154 \pm 0.024$/GPa for two different composite types, both linear in the measurement range of 40 MPa and 100 Mpa, respectively. The stress coefficient is similar to the direct stress optic coefficient that describes stress-induced birefringence in photoelasticity. In the case of CFRP, the effect we observe is attributed to changes in the refractive index of the effective medium comprising the carbon fibers in the polymer matrix. The stress coefficient is therefore not a property of a general material, but rather the response to stress of a particular composite type. The results show that it is possible to correlate changes in reflected power with CFRP internal stress states. Therefore, this technique could be applied to quality assurance applications for CFRP manufacture, as well as structural health monitoring of in-service CFRP aerospace or automotive parts, where variations in the reflected power across the surface give a qualitative indication of the location of defects.

**Funding.** Engineering and Physical Sciences Research Council (EPSRC) (EP/N018249/1).

**Acknowledgment.** Relevant research data presented in this publication can be accessed at http://dx.doi.org/10.17861/b62fdb79-12f0-45ac-b8b7-f71d67134c4e.

## REFERENCES

1. C. Soutis, "Carbon fiber reinforced plastics in aircraft construction," Mater. Sci. Eng. A **412**, 171–176 (2005).
2. H. Adam, "Carbon fibre in automotive applications," Mater. Des. **18**, 349–355 (1997).
3. S. Kendrew, P. Doel, D. Brooks, A. M. King, C. Dorn, C. Yates, R. M. Dawn, I. Richardson, and G. Evans, "Prototype carbon fiber composite deformable mirror," Opt. Eng. **46**, 094003 (2007).
4. C. E. Bakis, L. C. Bank, V. L. Brown, E. Cosenza, J. F. Davalos, J. J. Lesko, A. Machida, S. H. Rizkalla, and T. C. Triantafillou, "Fiber-reinforced polymer composites for construction—state-of-the-art review," J. Compos. Constr. **6**, 73–87 (2002).
5. P. P. Parlevliet, H. E. N. Bersee, and A. Beukers, "Residual stresses in thermoplastic composites—a study of the literature—Part I: formation of residual stresses," Composites Part A **37**, 1847–1857 (2006).
6. P. P. Parlevliet, H. E. N. Bersee, and A. Beukers, "Residual stresses in thermoplastic composites—a study of the literature—Part II: experimental techniques," Composites Part A **38**, 651–665 (2007).
7. P. P. Parlevliet, H. E. N. Bersee, and A. Beukers, "Residual stresses in thermoplastic composites—a study of the literature—Part III: effects of thermal residual stresses," Composites Part A **38**, 1581–1596 (2007).
8. K. D. Cowley and P. W. R. Beaumont, "The measurement and prediction of residual stresses in carbon-fibre/polymer composites," Compos. Sci. Technol. **57**, 1445–1455 (1997).
9. G. Zhou and L. M. Sim, "Damage detection and assessment in fibre-reinforced composite structures with embedded fibre optic sensors—review," Smart Mater. Struct. **11**, 925–939 (2002).
10. C. Balasingh and V. Singh, "Measurement of residual stresses in CFRP laminates by x-ray diffraction method," Bull. Mater. Sci. **20**, 325–332 (1997).
11. S. J. Park and Y. S. Jang, "X-ray diffraction and x-ray photoelectron spectroscopy studies of Ni-P deposited onto carbon fibre surfaces: impact properties of a carbon-fibre-reinforced matrix," J. Colloid Interface Sci. **263**, 170–176 (2003).
12. K. D. Cowley and P. W. R. Beaumont, "Damage accumulation at notches and the fracture stress of carbon-fibre/polymer composites: combined effects of stress and temperature," Compos. Sci. Technol. **57**, 1211–1219 (1997).
13. A. S. Nielsen and R. Pyrz, "A novel approach to measure local strains in polymer matrix systems using polarised Raman microscopy," Compos. Sci. Technol. **62**, 2219–2227 (2002).
14. C. D. Stoik, M. J. Bohn, and J. L. Blackshire, "Nondestructive evaluation of aircraft composites using transmissive terahertz time domain spectroscopy," Opt. Express **16**, 17039–17051 (2008).

15. B. Han, D. Post, and P. Ifju, "Moiré interferometry for engineering mechanics: current practices and future developments," J. Strain Anal. Eng. Des. **36**, 101–117 (2001).
16. J. P. McCrory, S. K. Al-Jumaili, D. Crivelli, M. R. Pearson, M. J. Eaton, C. A. Featherston, M. Guagliano, K. M. Holford, and R. Pullin, "Damage classification in carbon fibre composites using acoustic emission: a comparison of three techniques," Composites Part B **68**, 424–430 (2015).
17. D. Crivelli, M. Guagliano, M. Eaton, M. Pearson, S. Al-Jumaili, K. Holford, and R. Pullin, "Localisation and identification of fatigue matrix cracking and delimitation in a carbon fibre panel by acoustic emission," Composites Part B **74**, 1–12 (2015).
18. T. Sakai, Y. Iihara, and S. Yoneyama, "Photoelastic stress analysis of the fiber/matrix interface in a single-fiber composite," J. Jpn. Soc. Exp. Mech. **14**, 110–115 (2014).
19. A. Pawlak, P. Zinck, A. Galeski, and J. F. Gerard, "Photoelastic studies of residual stresses around fillers embedded in an epoxy matrix," Macromol. Symp. **169**, 197–210 (2001).
20. Z. Li and Z. Meng, "A review of the radio frequency non-destructive testing for carbon-fibre composites," Meas. Sci. Rev. **16**, 68–76 (2016).
21. P. Schemmel, G. Deiderich, and A. J. Moore, "Direct stress optic coefficients for YTZP ceramic and PTFE at GHz frequencies," Opt. Express **24**, 8110–8119 (2016).
22. P. Schemmel, G. Deiderich, and A. J. Moore, "Measurement of direct strain optic coefficient of YSZ thermal barrier coatings at GHz frequencies," Opt. Express (submitted).
23. E. Hecht, *Optics*, 4th ed. (Addison-Wesley, 2001).
24. E. Tuncer, N. Bowler, and I. J. Youngs, "Application of the spectral density function method to a composite system," Physica B **373**, 306–312 (2006).
25. V. Myroshnychenko and C. Brosseau, "Effective complex permittivity of two-phase random composite media: a test of the two exponent phenomenological percolation equation," J. Appl. Phys. **103**, 084112 (2008).
26. J. Pearce and D. M. Mittleman, "Propagation of single-cycle terahertz pulses in random media," Opt. Lett. **26**, 2002–2004 (2001).